J|A|C|S
COMMUNICATIONS

Published on Web 08/31/2005

Superhydrophobic Perpendicular Nanopin Film by the Bottom-Up Process

Eiji Hosono,[†] Shinobu Fujihara,[‡] Itaru Honma,[†] and Haoshen Zhou*,[†]

National Institute of Advanced Industrial Science and Technology, Umezono, 1-1-1, Tsukuba 305-8568, Japan, and Keio University, 3-14-1, Hiyoshi, Kohoku-ku, Yokohama 223-8522, Japan

Received June 8, 2005; E-mail: hs.zhou@aist.go.jp

In recent years, the study of superhydrophobic materials, including their wetting−dewetting tendencies,[1] with a water contact angle (CA) larger than 150° has been the focus of many researchers.[2−7] The water contact angle is based on the water-repellent behavior of the fractal micro- and nanostructure of the material. Generally, preparation of the rough surface and subsequent coating of the surface with low surface energy molecules are essential processes in fabricating superhydrophobic materials. The trapping of air components in the surface fractal structure causes an increase in the water CA according to Cassie's law.[8]

$$\cos\theta_c = \Phi_1 \cos\theta_1 + \Phi_2 \cos\theta_2 \quad (1)$$

θ_c is the superficial contact angle; θ_1 and θ_2 are the contact angles of the flat films of components 1 and 2, respectively; and Φ_1 and Φ_2 are the surface area fractions of components 1 and 2, respectively. When component 2 is the air component with a water CA of 180°, eq 1 is expressed as eq 2.

$$\cos\theta_c = \Phi_1(\cos\theta_1 + 1) - 1 \quad (2)$$

This equation means that materials with small Φ_1 and large θ_1 will exhibit superhydrophobic properties.

The reported fabrication processes of fractal micro- and nanostructures with small Φ_1 are generally top-down processes, such as etching by lithography[9−12] or a self-assembly process using a polymer.[13] However, these processes cannot be controlled on the scale of several nanometers. Therefore, many of the reported superhydrophobic materials with water CAs larger than 170° are based on molecules with original water CAs larger than 90°, which are classified as hydrophobic.[4] This includes fluoroalkylsilanes and in general is based on the concept of a large θ_1.[14] To date, a fabrication process on the order of several nanometers with a very small Φ_1 has not been reported.

We notice from eq 2 that if a material with a very low Φ_1 (about 6×10^{-4}) is fabricated, a superhydrophobic material with a water CA around 180° can be fabricated even using materials with a low original water CA of around 70°, which is classified as hydrophilicity.[4] To fabricate very low Φ_1 materials, it is assumed that a bottom-up process instead of a top-down process is suitable. Recently, bottom-up processes have been applied to the fabrication of superhydrophobic surfaces. It was reported that a polyacrylonitrile nanofiber used as an anodic aluminum oxide template had a water CA of around 174°.[15] This is a very high CA. However, control of this material on the order of several nanometers is not possible because of the large Φ_1, 0.967. When carbon nanotube (CNT) films were used for a superhydrophobic surface, Φ_1 was relatively small, 0.06.[16] However, there are two problems in this case: the use of a multiwall CNT with a diameter of several tens of nanometers, and dense films. A decrease in Φ_1 is not expected when using the multiwall CNT. We selected the bottom-up process of high crystalline materials such as metal oxide and hydroxide based on chemical bath deposition (CBD).[17−20] If we could fabricate high crystalline materials with a needle morphology, we could control the size of these materials because the top of a fabricated single-crystalline needle consists of a small amount of atoms. The CBD method can be used to fabricate a single crystalline-like metal hydroxide and metal oxides because each metal complex in the solution is singly deposited on the substrate surface based on thermodynamics equilibrium conditions as a construction component of the crystals in the system. In this work, the fabrication of superhydrophobic materials with a water CA of 178° is reported, which is the highest CA to our knowledge, using a perpendicular nanopin film fabricated using a bottom-up process.

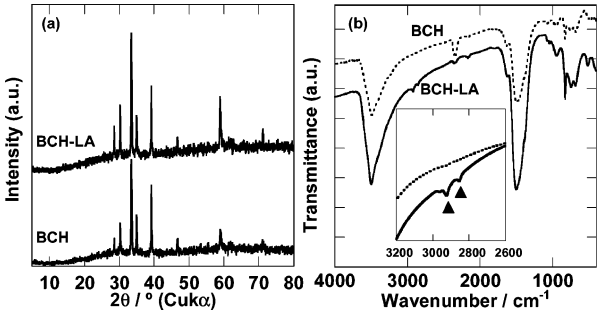

Figure 1. (a) XRD patterns of BCH and BCH-LA films. (b) FT-IR spectra of BCH and BCH-LA films.

Solutions for the CBD process were prepared by dissolving $CoCl_2 \cdot 6H_2O$ (0.15 mol/dm^3) and NH_2CO (5 g) in water (25 mL). Commercial borosilicate glass slides 1 mm in thickness were used as substrates for deposition. The substrates were put into bottles filled with the solutions, sealed, and kept at 60 °C for 24 h in a drying oven. Following the deposition, the deposited brucite-type cobalt hydroxide (BCH, $Co(OH)_{1.13}Cl_{0.09}(CO_3)_{0.39} \cdot 0.05H_2O$) films[20] were rinsed with ethanol and then dried at room temperature. The BCH films were then put into bottles filled with sodium laurate aqueous solutions (0.1 mol/dm^3) to coat the BCH surfaces with lauric acid, sealed, and kept at 60 °C for 5 h in a drying oven. After immersion, the fabricated films (BCH-LA) were rinsed with ethanol and then dried at room temperature.

We confirmed the crystal structure of BCH and lauric acid-coated BCH-LA films by X-ray diffraction (XRD). The crystal structure of BCH-LA was similar to that of the original BCH shown in Figure 1a. The FT-IR spectra in Figure 1b show the presence of the lauric acid. The peaks at 2855 and 2924 cm^{-1} were identified as the symmetric and asymmetric vibrations of $-CH_2-$ and $-CH_3-$ groups of the lauric acid, respectively.[21] Figure 2a,b shows the field-emission scanning electron microscope (FE-SEM) images of the BCH-LA films observed from the top and side, respectively. We can see a few scattered needles with a conelike morphology, which

[†] National Institute of Advanced Industrial Science and Technology.
[‡] Keio University.

10.1021/ja053745j CCC: $30.25

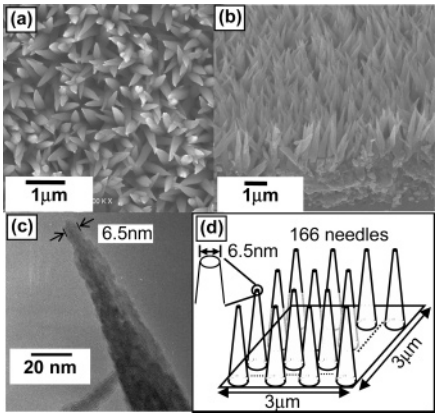

Figure 2. (a,b) FE-SEM images of the BCH-LA films observed from the top and side, respectively. (c) TEM images of the BCH-LA films. (d) A simple model of the film with the fractal structure.

are almost perpendicular to the surface of the glass substrate. The morphology of the BCH-LA films was not different from that of the BCH films[20] (see Supporting Information, Figure S1). Judging from these results, the immersion of a BCH film into a sodium laurate solution results in coating lauric acid on the BCH surface without changing the crystal structure. Figure 2c shows the transmission electron microscope (TEM) image of the top of a needle. The image indicates that the top of the needle is very sharp, with a diameter of 6.5 nm. It is believed that the bottom-up process, which is based on the piling up of each molecule individually, makes it possible to control the morphology on the order of several nanometers. To decrease the value of Φ_1, decreasing the area of the top of the film is important. Hence, to obtain a needle with a high mechanical strength and adhesiveness, the needle must be thick at the base. This is considered an ideal morphology for a superhydrophobic film.

We calculated the theoretical water CA in the case of a film like this. The number of needles, which is based on the image in Figure 2a, in $3 \times 3\ \mu m^2$ is 166. The diameter of each nanopin is 6.5 nm from the TEM image in Figure 2c. This film is expressed in Figure 2d as a simple model. The resultant value of Φ_1 is 6.12×10^{-4}. The water contact angle (θ_1) of the flat films of lauric acid is $75.2 \pm 6.6°$.[22,23] According to eq 2, the calculated water CA of this film is $177.8 \pm 0.1°$.

Figure 3c shows an image of the water on the BCH-LA film. We can see the almost perfect sphere made by the water. The water CA in this image is 178°. This value agrees with the calculated value. Therefore, it is possible to fabricate a superhydrophobic film with a water CA of around 180° according to this concept using a bottom-up process with high crystalline materials. The superhydrophobicity of this material was maintained after 12 h (see Supporting Information, Figure S2). Figure 3b,c shows the environmental scanning electron microscope (E-SEM) images of the water on BCH-LA films observed from the top and side, respectively. A perfect water sphere, which is similar to that in Figure 3a, is observed in both images. The change in the water morphology during wetting−dewetting was observed by E-SEM (see Supporting Information, Figure S3).

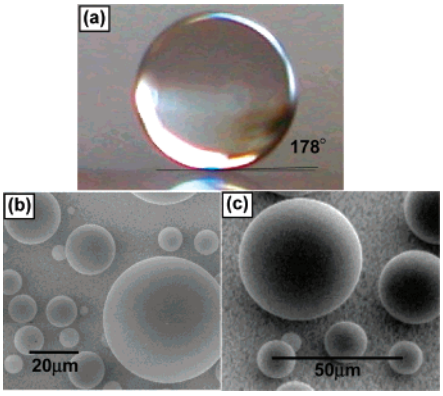

Figure 3. (a) Image of the water on a BCH-LA film. (b,c) E-SEM images of the water on BCH-LA films observed from the top and side, respectively.

In summary, we obtained a superhydrophobic surface with a water CA of 178° based on the concept of a small Φ_1 even with the low θ_1 of $75.2 \pm 6.6°$ by using a bottom-up process based on metal hydroxides. This result indicates a suitable application for control of real nanoscale processing using a solution synthesis method based on thermodynamics equilibrium conditions.

Supporting Information Available: Figures S1−S3. This material is available free of charge via the Internet at http://pubs.acs.org.

References

(1) Sharma, R. *Colloids Surf.* **1985**, *16*, 87−91.
(2) Erbil, H. Y.; Demirel, A. L.; Acvi, Y.; Mert, O. *Science* **2003**, *299*, 1377−1380.
(3) Fu, Q.: Rao, G. V. R.; Basame, S. B.; Keller, D. J.; Artyushkova, K.; Fulghum, J. E.; Lopez, G. P. *J. Am. Chem. Soc.* **2004**, *126*, 8904−8965.
(4) Blossey, R. *Nat. Mater.* **2003**, *2*, 301−306.
(5) Gu, Z. Z.; Uetsuka, H.; Takahashi, K.; Nakajima, R.; Onishi, H.; Fujishima, A.; Sato, O. *Angew. Chem., Int. Ed.* **2003**, *42*, 894−897.
(6) Han, J. T.; Lee, D. H.; Ryu, C. Y.; Cho, K. *J. Am. Chem. Soc.* **2004**, *126*, 4796−4797.
(7) Sun, T.; Wang, G.; Liu, H.; Feng, L.; Jiang, L.; Zhu, D. *J. Am. Chem. Soc.* **2003**, *125*, 14996−14997.
(8) Cassie, A. B. D.; Baxter, S. *Trans. Faraday Soc.* **1944**, *40*, 546−561.
(9) Shiu, J. Y.; Kuo, C. W.; Chen, P.; Mou, C. Y. *Chem. Mater.* **2004**, *16*, 561−564.
(10) Haynes, C. L.; Van Duyne, R. P. *J. Phys. Chem. B* **2001**, *105*, 5599−5611.
(11) Yoshimitsu, Z.; Nakajima, A.; Watanabe, T.; Hashimoto, K. *Langmuir* **2002**, *18*, 5818−5822.
(12) Yabu, H.; Takebayashi, M.; Tanaka, M.; Shimomura, M. *Langmuir* **2005**, *21*, 3235−3237.
(13) Wang, Y.; Liu, Z.; Han, B.; Sun, Z.; Zhang, J.; Sun, D. *Adv. Funct. Mater.* **2005**, *15*, 655−663.
(14) Feng, L.; Li, S.; Li, Y.; Li, H.; Zhang, L.; Zhai, J.; Song, Y.; Liu, B.; Jiang, L. Zhu, D. *Adv. Mater.* **2002**, *14*, 1857−1860.
(15) Feng, L.; Li, S.; Li, H.; Zhai, J.; Song, Y.; Jiang, L.; Zhu, D. *Angew. Chem., Int. Ed.* **2002**, *41*, 1221−1223.
(16) Li, H.; Wang, X.; Song, Y.; Liu, Y.; Li, Q.; Jiang, L.; Zhu, D. *Angew. Chem., Int. Ed.* **2001**, *40*, 1743−1746.
(17) Bunker, B. C.; Rieke, P. C.; Tarasevich, B. J.; Campbell, A. A.; Fryxell, G. E.; Graff, G. L.; Song, L.; Liu, J.; Virden, W.; McVay, G. L. *Science* **1994**, *264*, 48−55.
(18) Hosono, E.; Fujihara, S.; Kakiuchi, K.; Imai, H. *J. Am. Chem. Soc.* **2004**, *126*, 7790−7791.
(19) Hosono, E.; Fujihara, S.; Kimura, T. *Langmuir* **2004**, *20*, 3769−3774.
(20) Hosono, E.; Fujihara, S.; Honma, I.; Zhou, H. *J. Mater. Chem.* **2005**, *15*, 1938−1945.
(21) Jing, Z. H.; Wu, S. H. *Mater. Chem. Phys.* **2005**, *92*, 600−603.
(22) Garoff, N.; Zauscher, S. *Langmuir* **2002**, *18*, 6921−6927.
(23) Yiannos, P. N. *J. Colloid Sci.* **1962**, *17*, 334−347.

JA053745J